

A ground penetrating radar survey at Hasloh in the Ellerbeker Rinne pilot area in the BurVal project

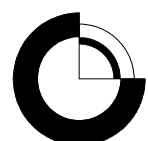
Data report

Ingelise Møller

A ground penetrating radar survey at Hasloh in the Ellerbeker Rinne pilot area in the BurVal project

Data report

Ingelise Møller



Contents

1.	Introduction	3
2.	The field experiment	4
2.1	The field sites	4
2.2	The data acquisition	5
2.3	Data editing and processing	7
3.	CMP's	8
4.	Reflection profile observations and interpretations	12
4.1	Observations	12
4.2	Interpretations.....	18
5.	Conclusions	22
6.	References	23

1. Introduction

A ground penetrating radar, GPR, survey is carried out at Hasloh in the Ellerbeker Rinne pilot area north of Hamburg, as part of the EU project, BurVal. The BurVal project, part-financed by the InterReg IIIb North Sea Programme of the European Union, is carried out with the purpose to deliver knowledge and understanding of the structural and hydrological properties of deeper groundwater resources found in buried valleys. This should lead to the development of spatial planning strategies that take these ancient groundwater reservoirs into account. In six pilot areas in The Netherlands, Germany and Denmark, buried valleys are extensively examined using geophysical and geological methods.

The aim of the GPR survey in the Ellerbeker Rinne Pilot Area is to test the applicability of GPR in the vulnerability mapping. GPR can provide information on detailed geological and sedimentological structures. Furthermore GPR can provide information on the water content in the ground.

Geoelectrical soundings and an electromagnetic EM31 profile have been acquired at the same site by Landesamt für Natur und Umwelt des Landes Schleswig-Holstein, LANU. These data indicate together with short hand drillings that clay till is deposited just below ground surface in the western part of the area and sandy deposits cover the rest of the area.

The GPR fieldwork is carried out 3-7 October 2005 during a week of sunny and dry weather. The week before heavy rain has moistened the ground and made the field muddy.

This report is primarily a data report, which list where and how the data are acquired, how data are processed and display the GPR profiles. The CMP data collected along profiles have not yet been processed as multi-fold GPR data. Only short comments on the results are provided. No description of the GPR method is given; such ones can be found in e.g., Davis & Annan (1989), Jol & Bristow (2003) and Neal (2004).

2. The field experiment

2.1 The field sites

The field site has been selected by LANU. The criteria for the field site were that the site should be situated in a geological setting, where both clays and sands are present just below ground surface. The survey area is a field bordered by a hedge of large trees and a forest to the south (Fig. 1). The field was covered with young rape plants.



Figure 1. Photo of the field site seen from west. The measuring poles seen in the photo mark the GPR lines.

At the field site data are acquired along four lines, which have an inline distance of about eleven meters (Fig. 2). The southernmost of the lines (L00 and L01) are located on the line, where other geophysical methods also are applied. The lengths of the lines are about 400 m. Furthermore, data are acquired along four short perpendicular lines of a length of 50-60 m. The aim of such a survey grid is to obtain sparse information on the 3D variation in the ground.

Along line L01 three areas are selected for multifold data collecting. A number of Common Mid Point, CMP, gathers are collected with a spacing of 0.5 m between the adjacent CMP's.

The line, along which L00 and L01 are acquired, was marked in the field by poles. The GPR profile distances are measured by an odometer wheel, while collecting the data. Furthermore, the line positions and CMP mid points are surveyed by a theodolite. The GPR profile lengths measured with the odometer wheel are not corrected to the actual distances measured with the theodolite.

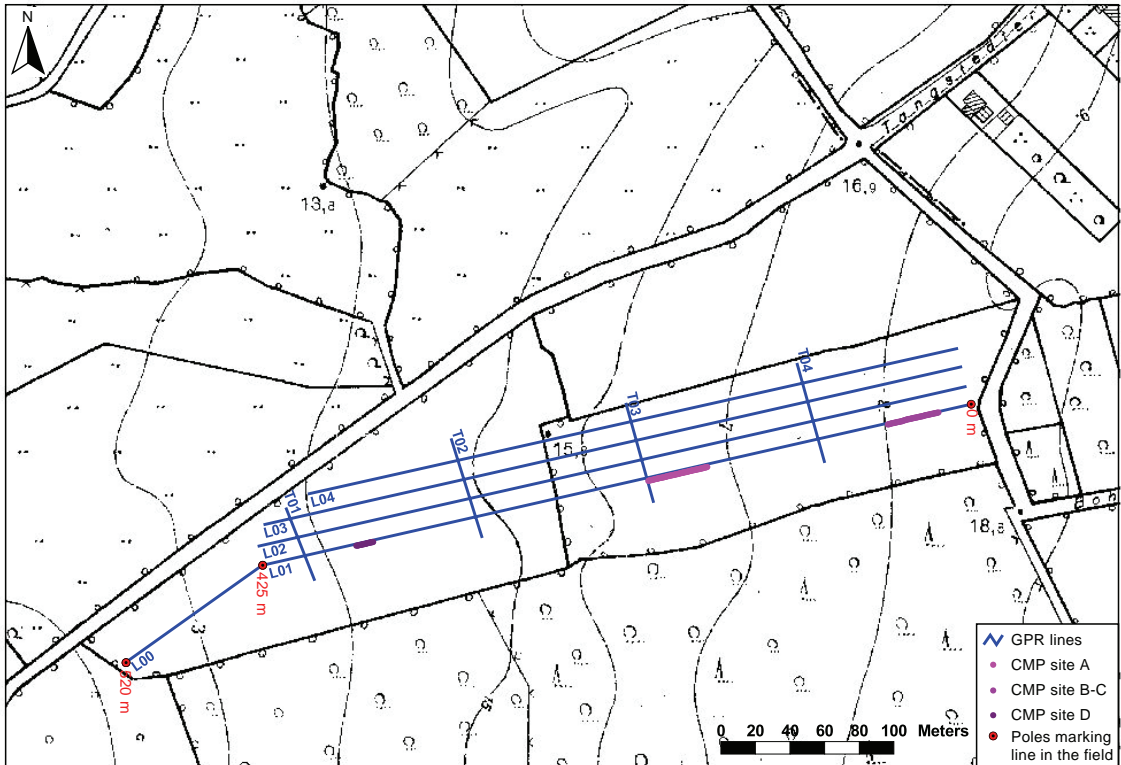


Figure 2. Map of GPR survey area with GPR lines and CMP profiles marked.

2.2 The data acquisition

The GPR data are acquired in step mode with a Sensors & Software pulseEKKO 100A system (Fig. 3). The system is equipped with a 400 V transmitter and antennae with a nominal centre frequency of 50 and 100 MHz. The nominal centre frequency of 100 MHz is chosen for the survey since experience show that this frequency is a good compromise between resolution and penetration. Data are also acquired using the nominal centre frequency of 50 MHz to obtain a better penetration depth. The specific data acquisition parameters are listed in Table 1.

Common mid point, CMP, soundings are carried out along three part of L01 (Fig. 4). The CMP soundings provide information on the velocity at the site. The position of the CMP profiles are selected at locations on the GPR profiles with different penetration depth. Data acquisition parameters for the CMP soundings are listed in Table 1.

Table 1. Data acquisition parameters for reflection mode and CMP soundings

Data acquisition parameter	Reflection mode	Reflection mode	CMP sounding
Nominal centre frequency	100 MHz	50 MHz	100 MHz
Transmitter voltage	400 V	400 V	400 V
Stepsize	0.3 m along profile	0.5 m along profile	0.3 m increase between antennae
Antennae separation	1.0 m	2.0 m	1.0 m (at start) to 6.5 m, 8 m or 10.1 m
Time window	600-800 ns	600 ns	500 ns
Sample distance along trace	0.8 ns	0.8 ns	0.8 ns
Stacks	16	16	32



Figure 3. Photo of GPR system in reflection mode. Data are collected along profile L01 seen from east.



Figure 4. Photo of GPR system in CMP mode. Data are collected at the eastern end of profile L01.

2.3 Data editing and processing

The data editing of the data in reflection mode includes that trace comments about line crossing are added and that some lines are reversed and repositioned, so all line distances increase from west towards east and from north towards south. The Time-zero is adjusted for all lines.

A standard processing is applied including a dewow reducing the inductive part of the signal, a low pass filtering reducing high frequency electromagnetic noise, a migration at constant velocity and a scaling of data by automatic gain control. The processing parameters are listed Table 2.

Table 2. *The data processing parameters.*

Processing procedure	Processing parameter
Dewow	
Lowpass filter	Cut of frequency 187 MHz (for 50 MHz data) and 250 MHz (for 100 MHz data)
Migration (constant velocity)	Velocity 0.09 m/ns
Gain	AGC, Gain-max=100, window of 4 pulses

The velocities are evaluated through a simple matching of reflection hyperbolas for selected CMP soundings using the software REFLEXW. According to the CMP's the rms velocities are varying between 0.07 m/ns to 0.09 m/ns, with a majority of the CMP's having rms velocities of about 0.09 m/ns. At a few CMP's the ground wave have a higher velocity of up to 0.12 m/ns. Since the most CMP's have rms velocities about 0.09 m/ns the profiles have been migrated using a velocity 0.09 m/ns.

The GPR profiles are displayed in Chapter 4. The profiles are displayed with a vertical exaggeration of 2 using a depth conversion with a velocity of 0.09 m/ns. The profiles have not been corrected for topography. One should take into account that the ground surface is dipping towards west as a plane.

3. CMP's

A few CMP's from each profile are displayed in Figs. 5–7. The CMP's are dewoed and gained by AGC. The CMP's at site D are furthermore bandpass filtered to reduce the high frequency noise. A straight line is matched to the direct airwave and the direct ground wave as well as reflection hyperbolas are matched to the reflections. The procedure is carried out in the software REFLEXW.

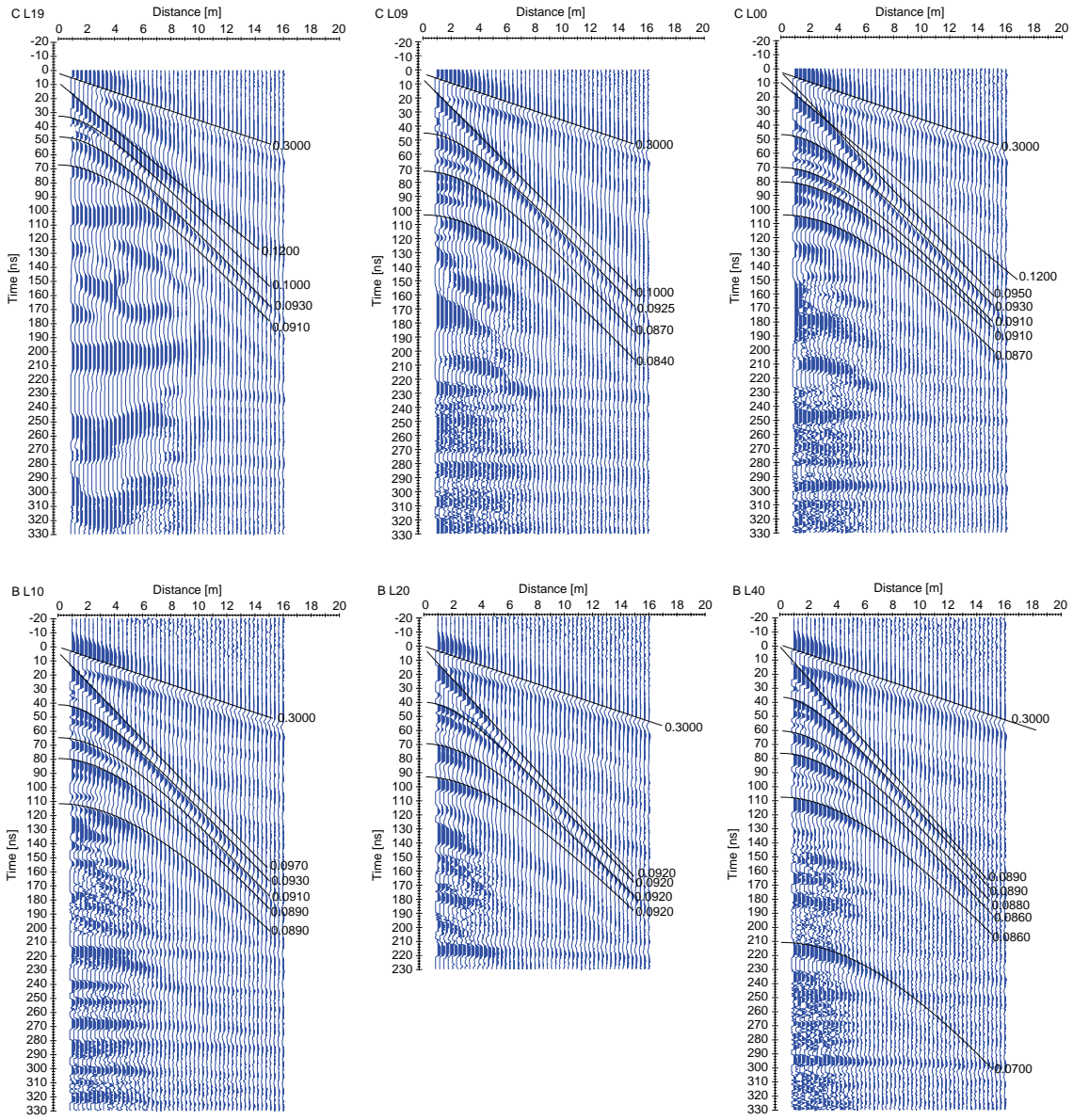


Figure 5. CMP's from site B and C.

The CMP's displayed in Fig. 5 are acquired in the eastern end of profile L01, where the best penetration depth is obtained. The rms velocities lie in between 0.084 m/ns and 0.093 m/ns except for one at 0.070 n/ns from a deep reflection at 210 ns. The velocity of the direct ground wave lies between 0.092 m/ns and 0.12 m/ns.

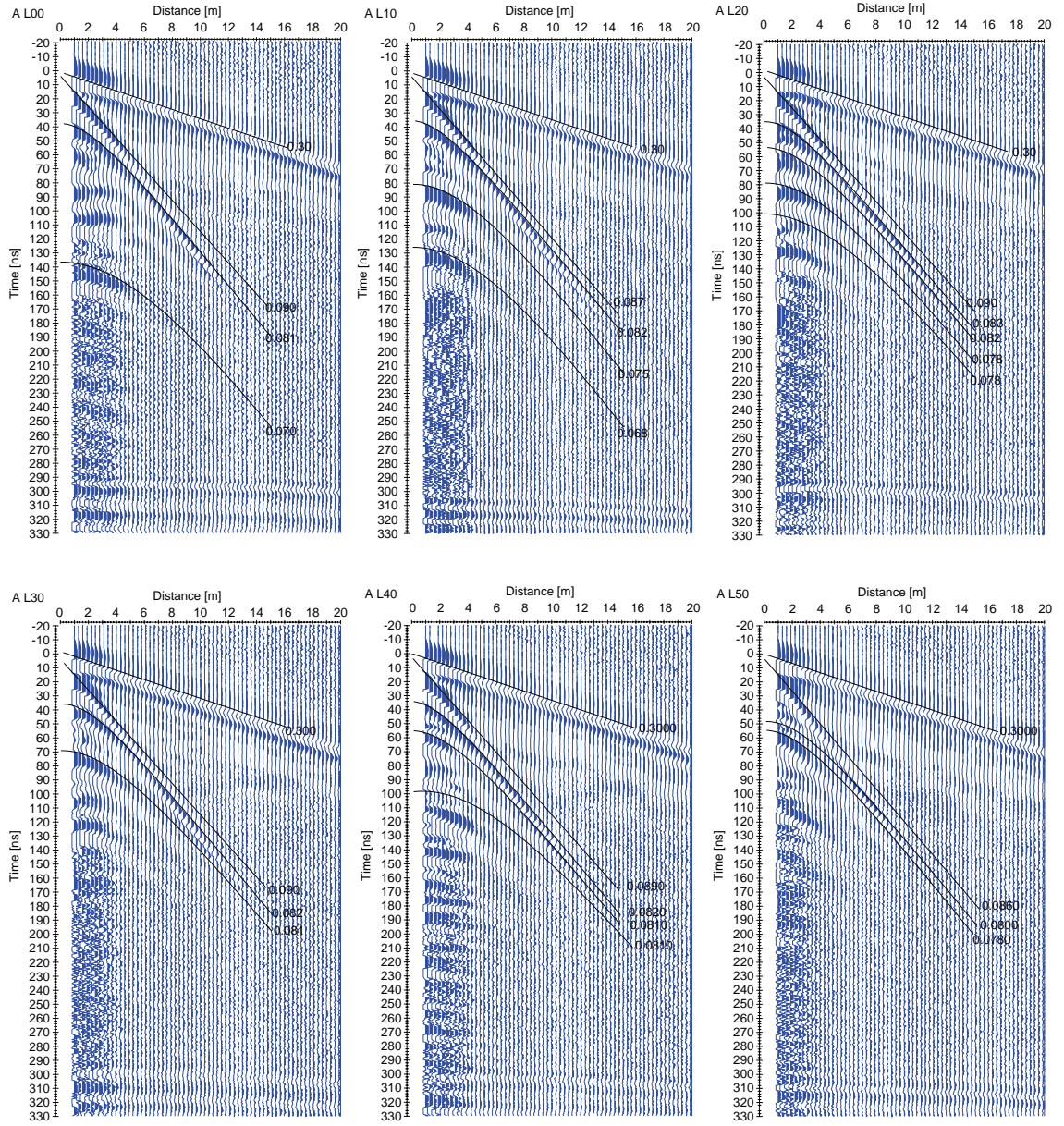


Figure 6. CMP's from site A.

The CMP's displayed in Fig. 6 are acquired in the middle of profile L01. The rms velocities lie in between 0.068 m/ns and 0.083 m/ns. The velocity of the direct ground wave lies between 0.086 m/ns and 0.09 m/ns. The velocities are in general a little less than at site B-C, especially for the reflections about 130 ns two-two-time.

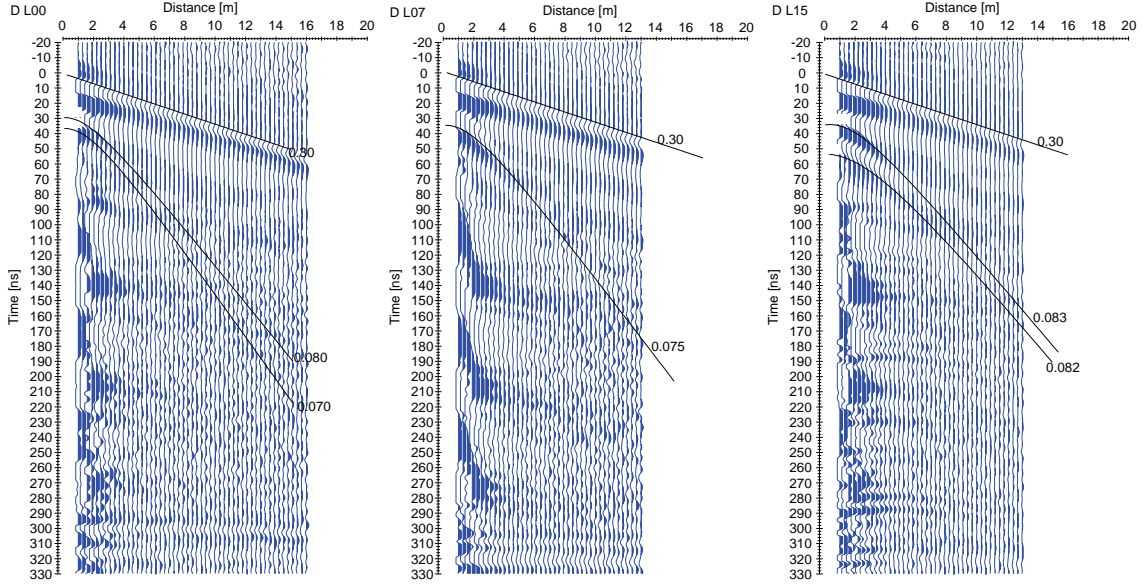


Figure 7. CMP's from site D.

The CMP's displayed in Fig. 7 are acquired in the western part of profile L01, where poor penetration depth is obtained. Only one or two reflections can be seen in the CMP before the signal is attenuated. The rms velocities lie in between 0.070 m/ns and 0.083 m/ns. No direct ground wave can be observed. The velocities are in general a little less than at site B-C, and similar to the ones at site A.

The water content can be estimated in a medium to coarse textured soil using Topp's relationship (Topp et al. 1980), when the interval velocities are determined. The interval velocities can be determined using Dix' analyses (Dix 1956).

In the eastern part of the field at CMP site B-C, the best penetration depth is obtained. Drillings carried out by LANU also showed that the near surface layers consisted of fine to medium sand. This means that Topp's relationship is valid for CMP's in site B-C. Table 3 shows interval velocity and water content estimates for CMP L40 in site B (Fig. 5).

Table 3. Estimated interval velocity, horizon depth, apparent dielectrical permittivity and water content for CMP L40 in site B. The rms-velocity and the intercept-time are found by matching a hyperbola to the CMP diagram (Fig. 5) using the program REFLEXW. The dielectrical permittivity is calculated assuming that the horizons consist of low-loss material.

Horizon	rms-velocity [m/ns]	Intercept time [ns]	Interval velocity [m/ns]	Depth [m]	Apparent dielectrical permittivity	Water content [%]
1	0.089	36	0.089	1.60	11.4	21.4
2	0.088	60	0.087	2.64	12.1	22.6
3	0.086	76	0.078	3.26	14.8	27.2
4	0.086	107	0.086	4.60	12.2	22.9
5	0.070	210	0.048	7.07	39.0	50.4

The estimated water content for Horizon 1-4 seem to be reasonable for a partly saturated soil, whereas the water content in Horizon 5 seems to be high even for a saturated soil as the porosity then should be 50 %. The interval velocity in Horizon 5 is also estimated to be low. A low velocity may also indicate that clays are present. Thus the estimate of dielectrical permittivity may not be valid, as it is calculated using the approximation valid for low-loss material. Furthermore, one have to take into account that even small uncertainties in the rms-velocity and the intercept-time may result in significant uncertainties in the interval velocity and depth estimate.

4. Reflection profile observations and interpretations

This chapter contains a description of the GPR profiles shown in Figs. 8–11. The descriptions are primarily based on Figs. 8 and 10, which display the GPR profiles obtained using the 100 MHz centre frequency. The profiles obtained using the 50 MHz centre frequency (Figs. 9–11) may display a little larger penetration depths particular in the eastern part of the field site as well as the deeper reflections look more continuous. The 50 MHz GPR profiles have a lower resolution.

Furthermore, a few interpretations solely based on the GPR profiles are given in the last part of the chapter. These interpretations are also illustrated on maps and GPR profiles. (Figs. 12–14).

4.1 Observations

GPR profile L00 (Figs. 8 and 9) is 95 m and is orientated SW-NE in the most western part of the field. Profile L00 ends at profile L01. The profile has a very poor penetration depth of about 60 ns (c. 2.7 m). Only a very weak reflection may be seen just below the direct waves. The large diffraction hyperbolas below 150 ns are caused by reflection through the air from trees at the border of the field.

GPR profile L01 (Figs. 8 and 9) is 413 m and is orientated E-W almost parallel to the forest bordering the field to the south. The profile has penetration depths between 60 ns (c. 2.7 m) in the most western part to about 200 ns (c. 9.0 m) in the eastern part. The penetration depth change rapidly from about 75 ns (c. 3.4 m) to about 175 ns (c. 7.9 m) at the profile distance 100 m. At this position apparently westward dipping reflections start to be seen toward the east in the profile (Fig. 13). The reflections are continuous, parallel and slightly undulation. The reflections in the topmost 50–75 ns (c. 2.3–3.4 m) are discontinuous and have a hummocky look. About profile distance 180–255 m a basin-like structure are seen reaching a depth about 100 ns (c. 4.5 m). In the eastern part of the profile east of 340 m the parallel reflections disappear and more hummocky and undulating reflections take over. The large diffraction hyperbolas below 175 ns are reflections from large trees south of the profile at the edge of the forest. At the very eastern end of the profile diffraction hyperbolas from trees just east of the profile are seen from 75 ns.

GPR profile L02 (Figs. 8 and 9) is 403 m and is orientated E-W parallel to L01. The profile has a similar appearance to GPR profile L01. The penetration depth varies from 60 ns (c. 2.7 m) in the western part of the profile to 225 ns (c. 10.1 m) in the eastern part of the profile with a dominating penetration depth about 175 (c. 7.9 m) ns in the middle part of the profile. The abrupt change in penetration depth appears about profile distance 100 m, where continuous parallel westward dipping reflections start. These reflections can be followed to the very eastern end of the profile (Fig. 13). The basin-like structure is less pronounced and can be seen between profile distance 185–245 m and down to a depth of 100

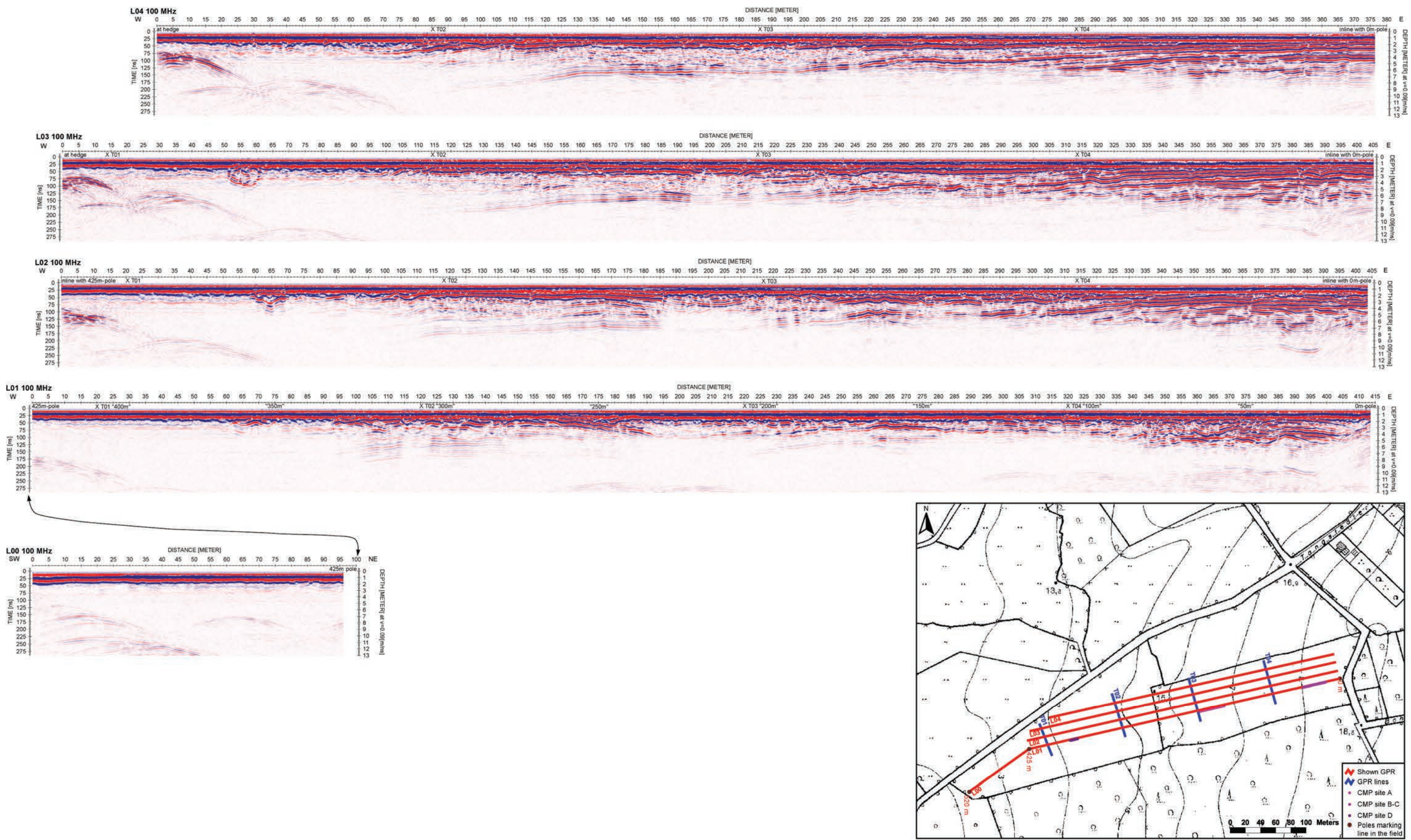


Figure 8. GPR profiles L00–L04 collected with 100 MHz centre frequency. The displayed profiles are marked in red on the map of the field site.

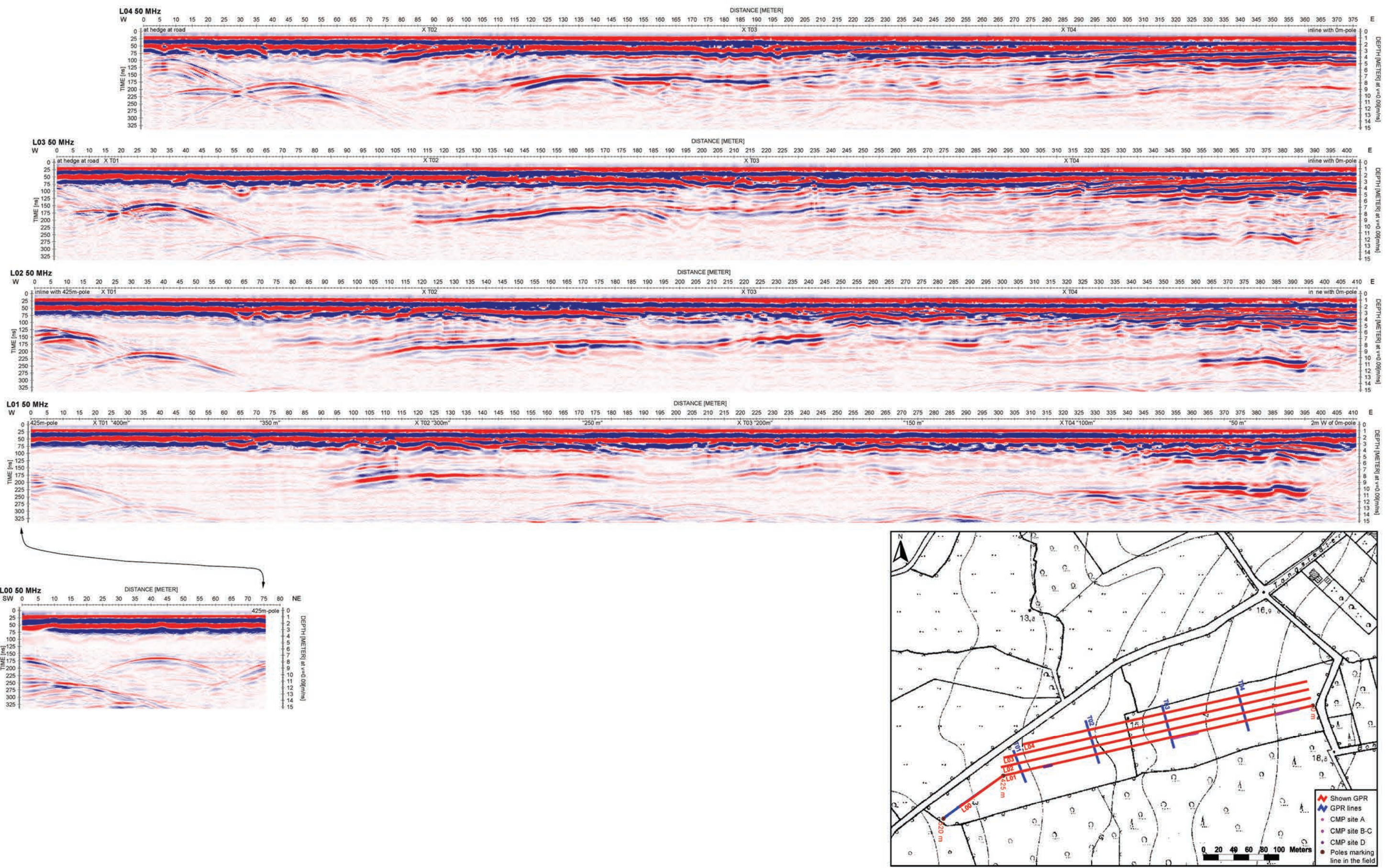


Figure 9. GPR profiles L00–L04 collected with 50 MHz centre frequency. The displayed profiles are marked in red on the map of the field site.

ns (c. 4.5 m). The large diffraction hyperbolas below 75 ns in the western end of the profile are caused by large trees in the hedge bordering the field NW of the profile.

GRR profile L03 (Figs. 8 and 9) is 405 m and is orientated E-W parallel to L01 and L02. The profile has a similar appearance to the other profiles. The penetration depth varies between 60 ns (c. 2.7 m) in the western end of the profile to 250 ns (c. 11.3 m) in the eastern part of the profile with the dominating penetration depth about 175 ns (c. 7.9 m) in the middle part of the profile. The rapid change in penetration depth occurs at profile distance 110 m, where the westward dipping continuous reflections start and continue to the very eastern end of the profile (Fig. 13). In the interval between 110–270 m discontinuous reflections with more hummocky appearance are seen between ground surface and the continuous reflections. The large diffraction hyperbolas in the western end of the profile are caused by large trees in the hedge bordering the field toward NV.

GPR profile L04 (Figs. 8 and 9) is 375 m and is orientated E-W parallel to L01, L02 and L03. The profile has a very similar appearance to L03. The penetration depth varies from 70 ns (c. 3.2 m) in the western part of the profile to about 200 ns (c. 9.0 m) in the eastern part of the profile with a dominating penetration depth about 175 ns (c. 7.9 m) in the middle of the profile. The abrupt change in penetration depth occurs at profile distance 90 m, where the westward dipping continuous reflections start. The continuous, parallel, dipping reflections continues to the very eastern end of the profile (Fig. 13). Between ground surface and the parallel continuous reflection discontinuous, more hummocky reflections are seen in the profile interval 90–220 m. The large diffraction hyperbolas in the western end of the profile are caused by large trees in the hedge bordering the field toward NV.

GPR profile T01 (Figs. 10 and 11) is 46 m and is orientated N-S perpendicular to profiles L01–L04. Profile T01 crosses profile L01–L03 about profile distance 20 m in the very western end of the profiles. The penetration depth is about 60–70 ns (c. 2.7–3.2 m). Only weak reflections are seen below the direct waves. The large diffraction hyperbolas in the northern end of the profile are caused by large trees in the hedge bordering the field just to the north of the profile.

GPR profile T02 (Figs. 10 and 11) is 60 m and is orientated N-S perpendicular to profiles L01–L04. Profile T02 crosses profile L01–L04 about profile distance 120 m. The penetration depth varies from about 125 ns (c. 5.6 m) in the northern part of the profile to 200 ns (c. 9.0 m) in the middle of the profile, where the parallel continuous reflections start to appear. In this profile the parallel continuous reflections that can be correlated to the perpendicular profiles has an apparent dip towards N (Fig. 13). Between the ground surface and the parallel continuous reflections the reflections are discontinuous and have a hummocky appearance.

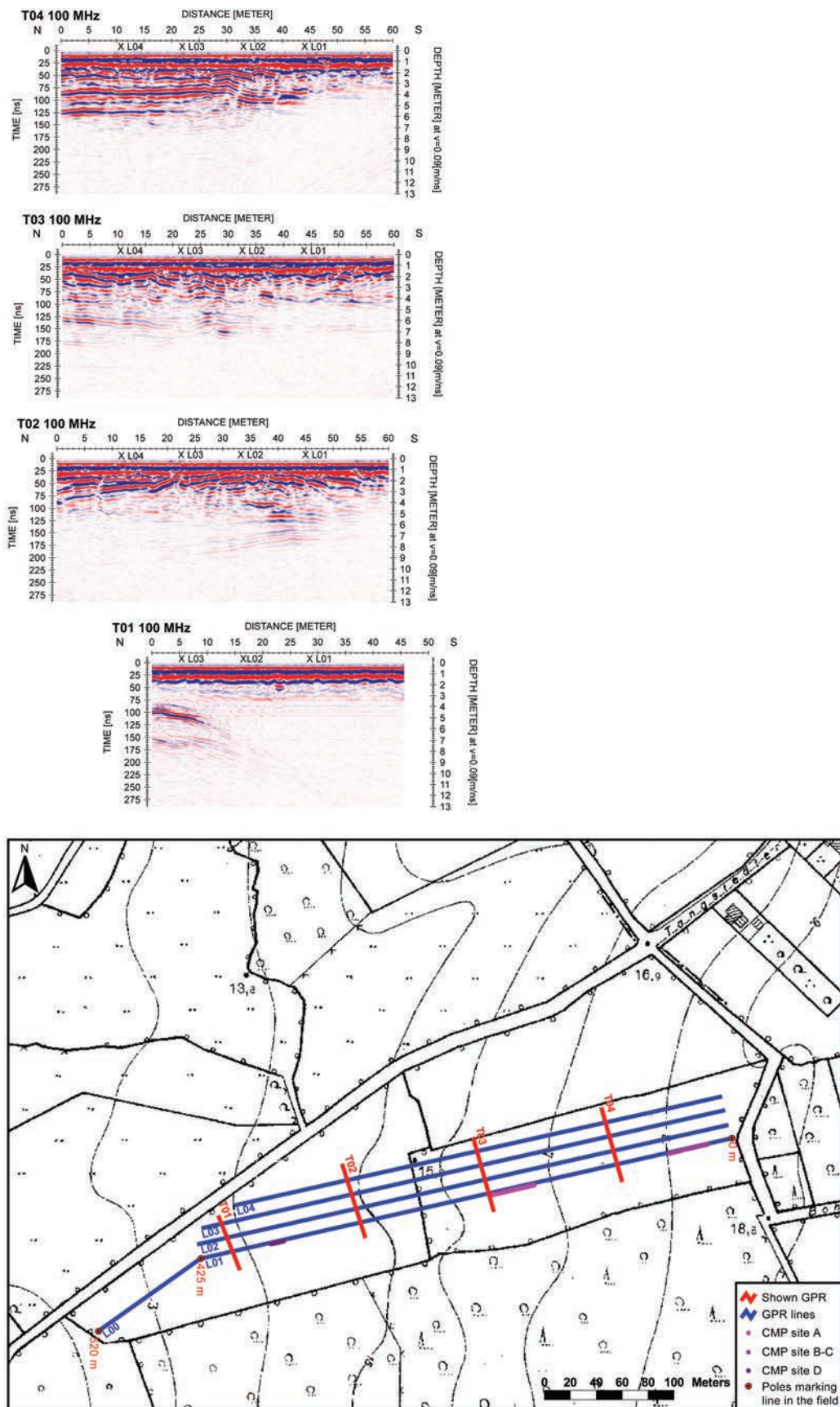


Figure 10. GPR profiles T01–T04 collected with 100 MHz centre frequency. The displayed profiles are marked in red on the map of the field site.

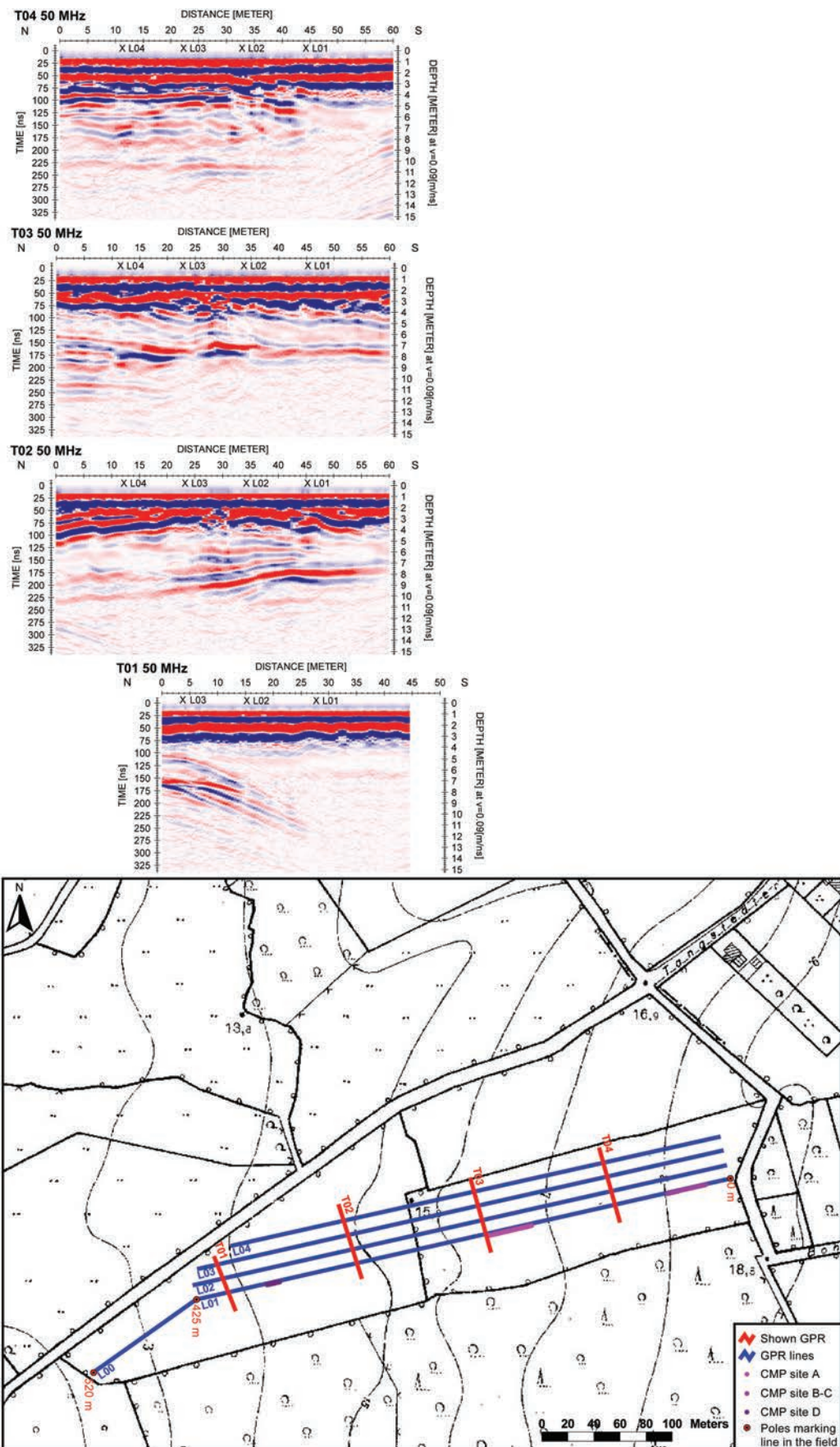


Figure 11. GPR profiles T01–T04 collected with 50 MHz centre frequency.

GPR profile T03 (Figs. 10 and 11) is 60 m and is orientated N-S perpendicular to profiles L01–L04. Profile T03 crosses profile L01–L04 about profile distance 220 m. The penetration depth is about 150 ns (c. 6.8 m). In this profile the parallel continuous reflections that can be correlated to the perpendicular profiles has north of profile distance 20 m an apparent dip slightly towards S (Fig. 13). In the rest of the profile toward south the continuous reflections lies horizontal. Between the ground surface and the parallel continuous reflections the reflections are discontinuous and have a hummocky appearance.

GPR profile T04 (Figs. 10 and 11) is 60 m and is orientated N-S perpendicular to profiles L01–L04. Profile T04 crosses profile L01–L04 about profile distance 320 m. The penetration depth varies from about 100 ns (c. 4.5 m) in the southern end of the profile to about 150 ns (c. 6.8 m) in the middle and northern part of the profile. In this profile the parallel continuous reflections that can be correlated to the perpendicular profiles have north of profile distance 30 m an apparent dip slightly towards N. At profile distance 30 m the continuous reflections sharply change apparent dip towards S (Fig. 13). South of profile distance 35 m discontinuous reflections with a hummocky appearance lies between the ground surface and the parallel continuous reflections. The parallel continuous reflections become very weak in the southern part of the profile.

4.2 Interpretations

Figure 12 shows a map of GPR lines added information on the penetration depth. In the western part of the field site a gray blue line marks the rapid change in penetration depth.

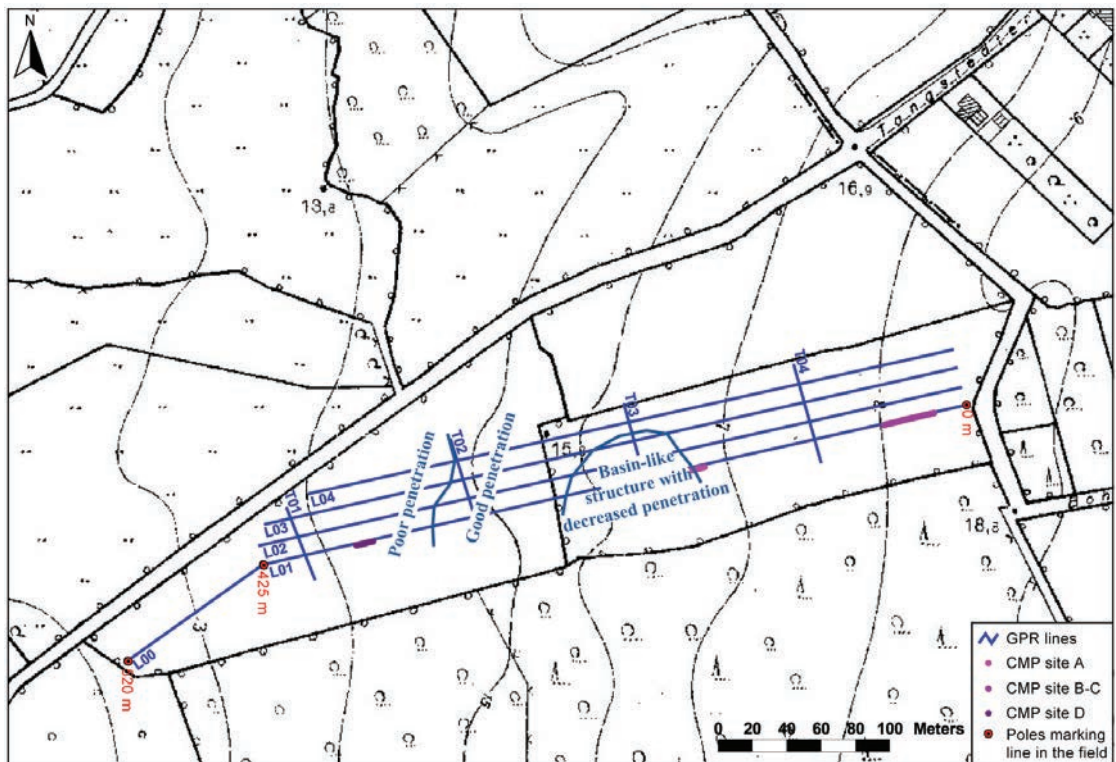


Figure 12. Map of GPR lines with changes in penetration depth marked by the gray blue line.

This line indicates that clay till are deposited just below the surface west of the line, where the penetration depth is poor. To the east of the line sandy deposits are deposited at ground surface and down to a depth at least as deep as the penetration depth.

The area with the basin-like structures seen in the GPR profiles L01–L03 is marked in Fig. 12. The basin-like structure may indicate that a lens of a different material is deposited at ground surface. The relatively weaker amplitudes and poorer penetration depth below the basin-like reflections indicate that the lens consists of a material with more fine-grained texture and most likely with higher clay content too. A lens of material with higher clay content and thus higher water content results in a lower velocity in the lens. A lower velocity pulls the reflections down, which means that the basin-like structure and the lens seem thicker than it actually may be. The CMP's at CMP site A, which partly lies with in the basin-like structure, results in slightly lower velocities than at site B-C in the more sandy eastern part of the field site.

In the most of the GPR profiles continuous westward dipping reflections are seen. The reflection that is deepest laying to the west is picked. This reflection can be correlated between profiles L01–L04 using profiles T02–T04. The picked reflection is shown on the profiles displayed in Fig. 13. The reflection has an apparent general dip of about 2° towards W in profiles L01–L04 taking into account that the ground surface also dips towards W with about 0.7° . The cross profiles T02–T04 show apparent dip towards N in the western part and a slightly southward apparent dip in the middle and eastern part of the profiles.

Figure 14 shows a contour map of the elevation of the surface spanned by the picked reflection in Fig. 13. To the west, where the reflection lies at 6 m a.m.s.l., it lies about 9 m below ground surface and to the east, where the reflection lies about 15 m a.m.s.l., it lies about 2.5 m below ground surface. From the contour lines it can be seen that the reflection has a dip towards WSW in the eastern part of the field site. In the western part of the field the dip changes to a westnorthwestward direction. In the middle part of the field site, the true dip of the reflection may be disturbed by the basin-like structure (Fig. 12), which most likely has a lower velocity.

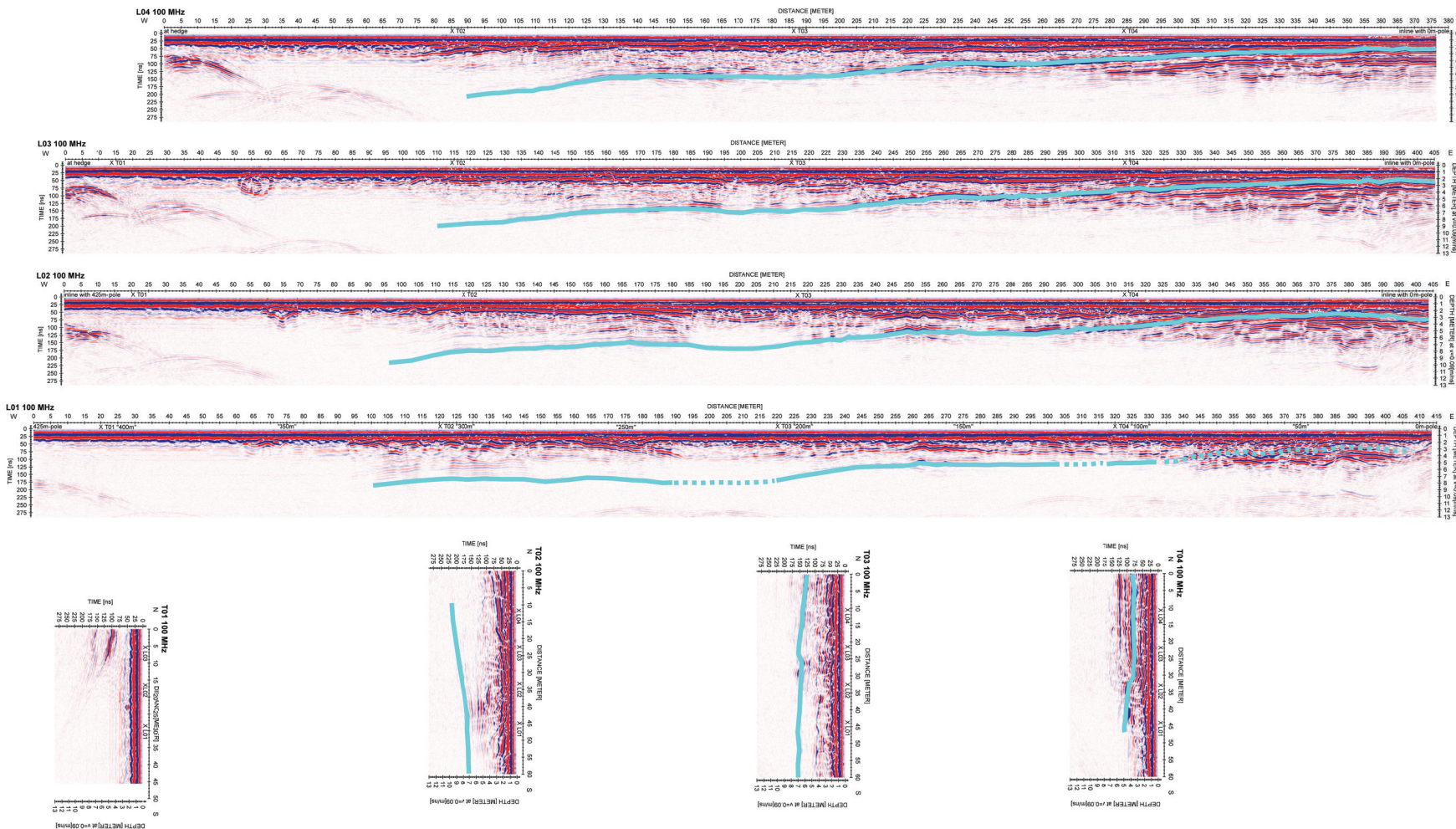


Figure 13. The GPR profiles L01-L04 and T01-T04 collected with 100 MHz. The cyan lines mark a dipping reflection that can be recognized in all GPR profiles.

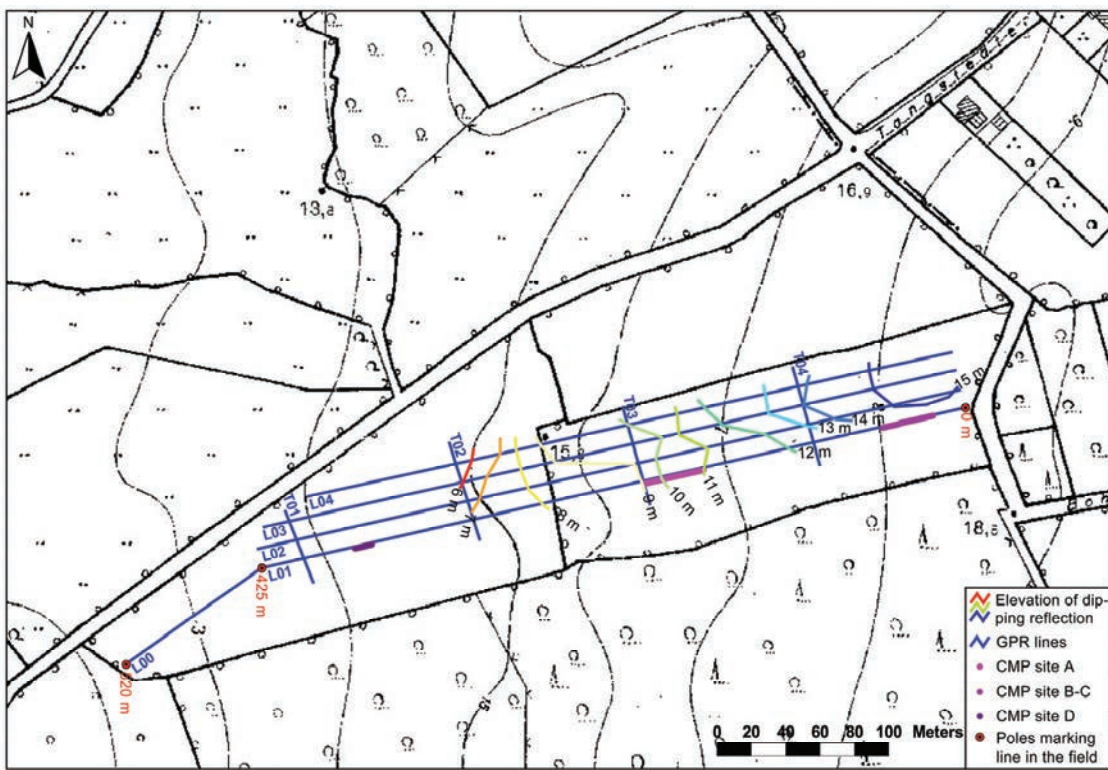


Figure 14. Contour map of the elevation of the dipping reflection picked in Fig. 13. The elevation is given in m a.m.s.l.

5. Conclusions

The GPR profiles are acquired in a field appointed by LANU for detailed vulnerability studies. About 1900 m of GPR profiles in a grid of parallel lines and tie-lines are obtained by both 50 MHz and 100 MHz GPR systems. Three short profiles of CMP gathers are also collected.

The GPR profiles provide information on sedimentary structures. Continuous dipping reflections are prominent. To some extend information on the distribution of clay till just below surface can be deduced from the penetration depth.

The information on velocities and thereby the dielectrical permittivity can be withdrawn from the CMP gathers. One example of estimation on water content is given.

6. References

- Davis, J.L. & Annan, A.P., 1989: Ground penetrating radar for high-resolution mapping of soil and rock stratigraphy. *Geophysical Prospecting* **37**, 531–551.
- Dix, C. H., 1956: Seismic Prospecting of Oil, Harper, New York.
- Jol, H.M. & Bristow, C.S., 2003: GPR in sediments: advice on data collection, basic processing and interpretation, a good practice guide. In: Bristow, C.S. & Jol, H.M. (eds.): *Ground penetrating radar in sediments*, Geological Society, London Special Publications **211**, 9–27.
- Neal, A., 2004: Ground-penetrating radar and its use in sedimentology: principles, problems and progress. *Earth-Science Reviews* **66**, 261–330.
- Topp, G. C., Davis, J. L. & Annan, A. P., 1980: Electromagnetic determination of soil water content: Measurements in coaxial transmission lines. *Water Resources Research* **16**, 574-582.